Available online at www.sciencedirect.com
SCIENCE DIRECT
Inorganica Chimica Acta 359 (2006) 1559–1572
Inorganica Chimica Acta
www.elsevier.com/locate/ica

Transition metal complexes with pyrazole derivatives as ligands

Susanne Bieller [a], Alireza Haghiri [a], Michael Bolte [a], Jan W. Bats [b], Matthias Wagner [a], Hans-Wolfram Lerner [a,*]

[a] Institut für Anorganische Chemie, Johann Wolfgang Goethe-Universität Frankfurt am Main, Marie-Curie-Straße 11, 60439 Frankfurt am Main, Germany
[b] Institut für Organische Chemie, Johann Wolfgang Goethe-Universität, Marie-Curie-Straße 11, 60439 Frankfurt, Germany

Received 30 September 2005; accepted 17 October 2005
Available online 7 December 2005

Abstract

Degradation reactions of scorpionates were observed in the presence of transition metal salts MX_2 to give complexes of transition metal and pyrazole derivatives. Otherwise, pyrazolato complexes of transition metals and weakly coordinating anions such as nitrates have been synthesized from transition metal nitrates and 3-phenyl- and 4-phenyldiazo-pyrazole. A number of complexes with pyrazole derivatives as ligands, $[Zn(3\text{-}t\text{BupzH})_2Cl_2]$, $[Fe_2(3\text{-Phpz})_6Cl_4]$, $[Cu(pzH)_4Br_2]$, $[Ni(py)_2(pzH)_2Cl_2]$, $[Li(THF)_4][Ti_2(\mu\text{-pz})_3Cl_4(NMe_2)_2]$, $[Zn_2(\mu\text{-3-Phpz})_2(3\text{-PhpzH})_2][(NO_3)_2]$, $[M(3\text{-PhpzH})_4(NO_3)_2]$ (M = Co, Ni, Cu, Zn, Cd), $[Zn(3\text{-PhpzH})_2(NO_3)_2]$, $[Zn(4\text{-PhN=NpzH})_2(NO_3)_2](H_2O)$, and $[Cd(4\text{-PhN=NpzH})_2(NO_3)_2(H_2O)_2]$, have been crystallized and characterized by single-crystal X-ray diffraction.

Keywords: Scorpionates; Pyrazole; Coordination chemistry; X-ray structure analysis

1. Introduction

Tris(1-pyrazolyl)borates (''scorpionates'') were invented by Trofimenko [1] more than 30 years ago and today are well established as ligands in coordination chemistry. Scorpionates with transition metals are now found useful in a wide range of chemistry from modelling the active site of metaloenzymes, through analytical chemistry and organic synthesis to catalysis and materials science [2].

Despite their widespread use, information regarding the degradation of these scorpionates is still rather limited (Fig. 1). Graziani et al. [3] described that the reaction between $FeCl_2$ and the Tl scorpionate, $Tl[t\text{BuB}(3\text{-}t\text{Bupz})_3]$, which led to deboronation of scorpionate anion to give *trans*-$FeCl_2(3\text{-}t\text{Bu-pzH})_4$.

The purpose of this paper is to give more detailed information about the reactivity of scorpionates towards transition metal halides. Moreover, we became interested in synthesis and characterization of transition metal complexes with pyrazole derivatives **3-R′pzH** and **4-R′pzH** as ligands with the intention to reverse degradation reactions of scorpionates.

2. Experimental

2.1. Synthesis of $[Zn(3\text{-}t\text{BupzH})_2Cl_2]$ (**1**)

A solution of fluorenyl scorpionate $C_{13}H_9B(3\text{-}t\text{Bupz})_3\text{-Li}\cdot\text{THF}$ [4] (0.13 g, 0.20 mmol) in a mixture of toluene (10 mL) and methylene chloride (5 mL) was added dropwise with stirring to a slurry of $ZnCl_2$ (0.03 g, 0.20 mmol) in methylene chloride (10 mL). After stirring for 8 h, the white precipitate was removed by filtration and the solvent was evaporated in vacuo. Recrystallization by slow diffusion of hexane to a chloroform solution gave colorless X-ray quality crystals.

2.2. Synthesis of $[Fe_2(3\text{-PhpzH})_6Cl_4]$ (**2**)

A solution of scorpionate $C_{13}H_9B(3\text{-Phpz})_3\text{Li}\cdot\text{THF}$ [4] (0.15 g, 0.21 mmol) in a mixture of toluene (10 mL) and

* Corresponding author. Tel.: +49 69 79829151; fax: +49 69 79829260.
E-mail address: lerner@chemie.uni-frankfurt.de (H.-W. Lerner).

0020-1693/$ - see front matter © 2005 Elsevier B.V. All rights reserved.
doi:10.1016/j.ica.2005.10.034

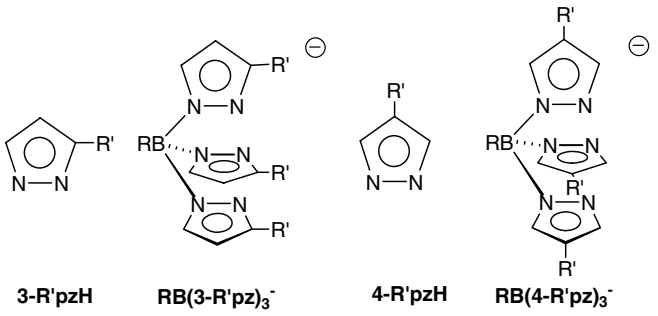

Fig. 1. Tris(1-pyrazolyl)borates, scorpionates.

methylene chloride (5 mL) was added dropwise with stirring to a slurry of $FeCl_2$ (0.03 g, 0.21 mmol) in methylene chloride (10 mL). After stirring for 8 h, the white precipitate was removed by filtration and the solvent was evaporated in vacuo. Recrystallization by slow diffusion of hexane to a chloroform solution gave colorless X-ray quality crystals.

2.3. Synthesis of [Cu(pzH)$_4$Br$_2$] (3)

p-$C_6H_4(B(tBu)pz_2Li)_2 \cdot 4THF$ [5] (0.18 g, 0.23 mmol) in THF (10 mL) was added dropwise with stirring to a solution of $CuBr_2$ (0.13 g, 0.46 mmol) in THF (15 mL), whereupon a green solution formed. The solvent was removed in vacuo, recrystallization of the green solid by slow diffusion of hexane to a THF solution gave blue crystals suitable for X-ray crystal structure analysis.

2.4. Synthesis of [Ni(py)$_2$(pzH)$_2$Cl$_2$] (4)

p-$C_6H_4(B(tBu)pz_2Li)_2 \cdot 4THF$ [5] (0.53 g, 0.68 mmol) in ethanol (10 mL) was added dropwise with stirring to a slurry of $[Ni(py)_4Cl_2]$ (0.61 g, 1.36 mmol) in ethanol (10 mL), whereupon a green solution and a yellow precipitate formed. The reaction mixture was stirred for 2 h at ambient temperature and the precipitate was removed by filtration. The remaining green solution was evacuated to dryness to give a turquoise solid. Colorless X-ray quality crystals were grown by slow diffusion of hexane to a ethanol solution of compound **3**. Yield: 0.08 g (0.19 mmol, 14%).

2.5. Synthesis of [Li(THF)$_4$][Ti$_2$(μ-pz)$_3$Cl$_4$(NMe$_2$)$_2$] ([Li][5])

A solution of *p*-$C_6H_4(B(t\text{Bu})pz_2Li)_2 \cdot 4THF$ [5] (0.73 g, 0.94 mmol) in THF (10 mL) was added at −78 °C to a

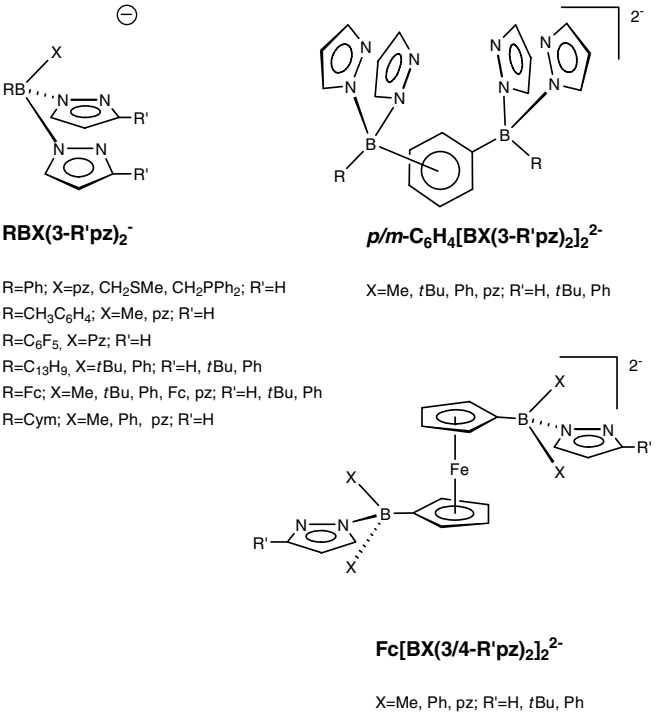

Fig. 2. (1-Pyrazolyl)borates, scorpionates.

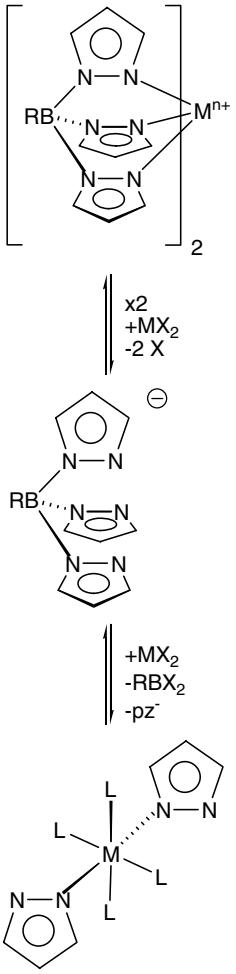

Scheme 1. Reaction of scorpionates with transition metal salts.

solution of $Ti(NMe_2)_2Cl_2$ (0.39 mg, 1.87 mmol) in THF (10 mL). After 1 h, stirring was continued at ambient temperature for 3 h, the solvent was reduced in vacuo to 5 mL and the solution was layered with pentane (15 mL) to form crystals of [**Li**][**5**] suitable for X-ray determination.

2.6. Synthesis of $[Zn_2(\mu\text{-}3\text{-}Phpz)_2(3\text{-}PhpzH)_2][(NO_3)_2]$ ([**6**][$(NO_3)_2$])

A solution of $Zn(NO_3)_2 \cdot 6H_2O$ (0.36 g, 0.14 mmol) in THF (10 mL) was added at ambient temperature to a solution of [FcB(3-$Phpz_3$)$_3$][Li(THF)] [6] (0.704 g, 1 mmol) in THF (50 mL). After 8 h of stirring at ambient temperature, the solvent was reduced in vacuo to 10 mL and the solution was layered with pentane (10 mL) to form crystals of [**6**][$(NO_3)_2$] suitable for X-ray determination.

2.7. Syntheses of $[M(3\text{-}PhpzH)_4(NO_3)_2]$ (M = Co, Ni, Cu, Zn, Cd) 7(**Co**), 7(**Ni**), 7(**Cu**), 7(**Zn**), and 7(**Cd**)

One equivalent of a transition metal nitrate as hydrate [$Co(NO_3)_2 \cdot 6H_2O$ (0.14 mmol); $Ni(NO_3)_2 \cdot 6H_2O$ (0.14 mmol); $Cu(NO_3)_2 \cdot 3H_2O$ (0.14 mmol); $Zn(NO_3)_2 \cdot 6H_2O$ (0.07 mmol) and $Cd(NO_3)_2 \cdot 6H_2O$ (0.14 mmol)] and 4 equivalents of 3-phenylpyrazole [7] were combined in ethanol (10 mL) under ambient conditions, forming a clear solution. Slow evaporation of the solvent led to deposition of X-ray quality crystals of pink **7**(**Co**), blue **7**(**Ni**), green **7**(**Cu**), colorless **7**(**Zn**), and colorless **7**(**Cd**).

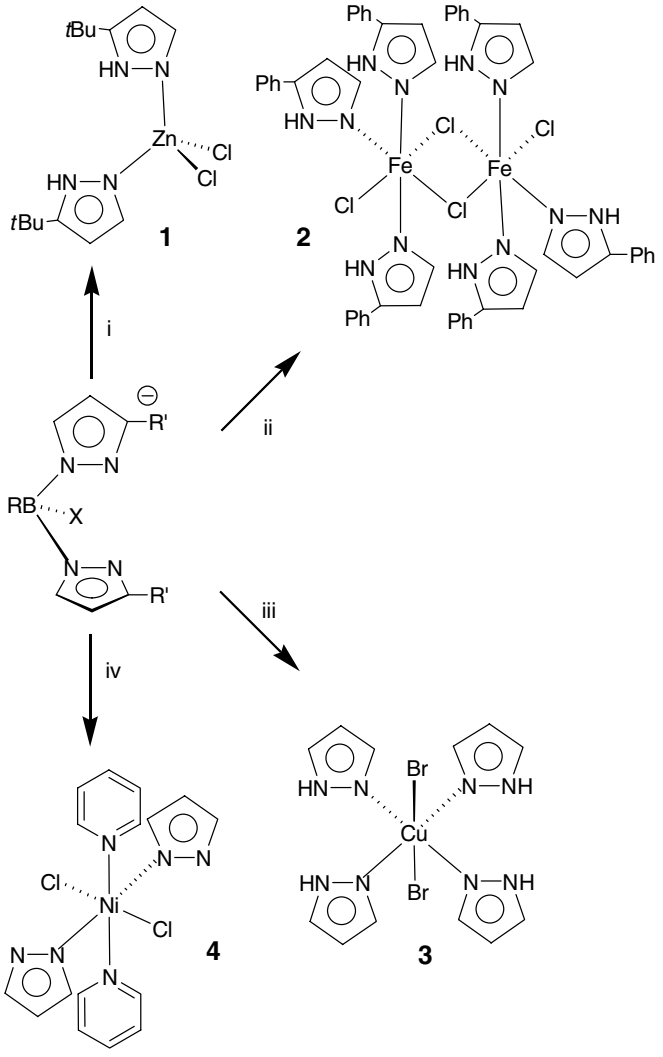

Scheme 2. Deboronation of scorpionates with bulky substituents; i: $+ZnCl_2/+H^+/-RBBr_2/-Cu^{2+}/-3\text{-}t$Bupzh, X = 3-*t*Bupz/R = $C_{13}H_9$/R′ = *t*Bu; ii: $+FeCl_2/+H^+/-RXBCl/-Fe^{2+}/-3$-PhpzH, X = 3-Phpz/R = $C_{13}H_9$/R′ = Ph; iii: $+CuBr_2/+H^+/-RXBBr/-Cu^{2+}/-$pzH, X = C_6H_4/R = *t*Bu/R′ = H; and iv: $+Ni(py)_2Cl_2/+H^+/-RXBBr/-Ni^{2+}/-$pzH, R = *t*Bu/X = C_6H_4/R = *t*Bu/R′ = H.

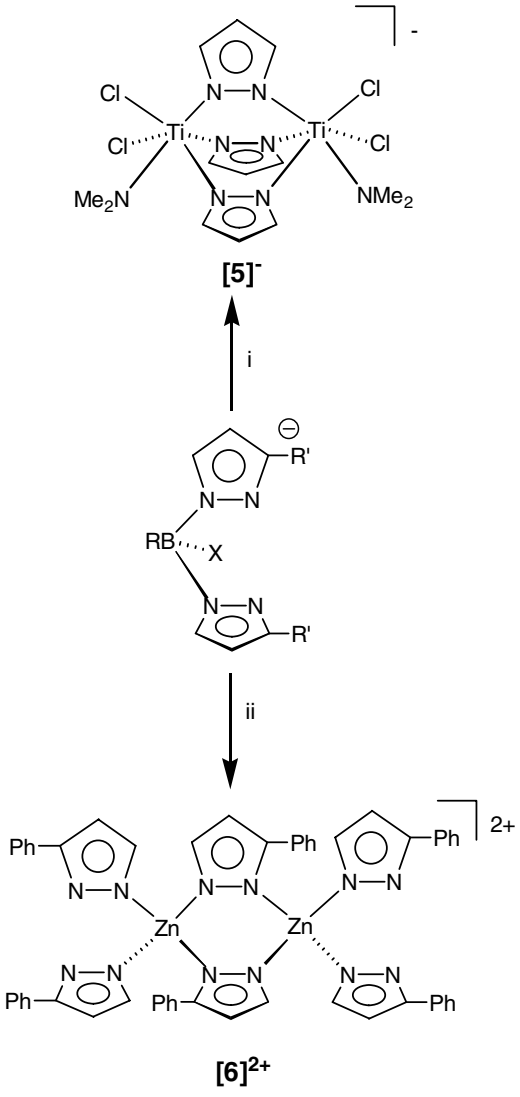

Scheme 3. Syntheses of the dinuclear complexes **Li**[**5**] and [**6**]$(NO_3)_2$; i: $+TiCl_2(NMe_2)_2/-RXBNMe_2/-$pz X = C_6H_4/R = *t*Bu/R′ = H; and ii: $+Zn(NO_3)_2/+H^+/-RXB$(3-Phpz), X = 3-Phpz/R = Fc/R′ = Ph.

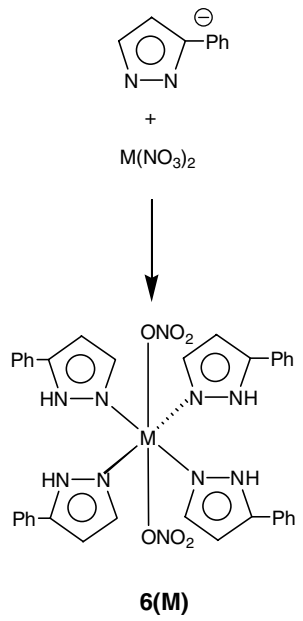

Scheme 4. Synthesis of pyrazolato complexes **7**(**Co**), **7**(**Ni**), **7**(**Cu**), **7**(**Zn**), and **7**(**Cd**).

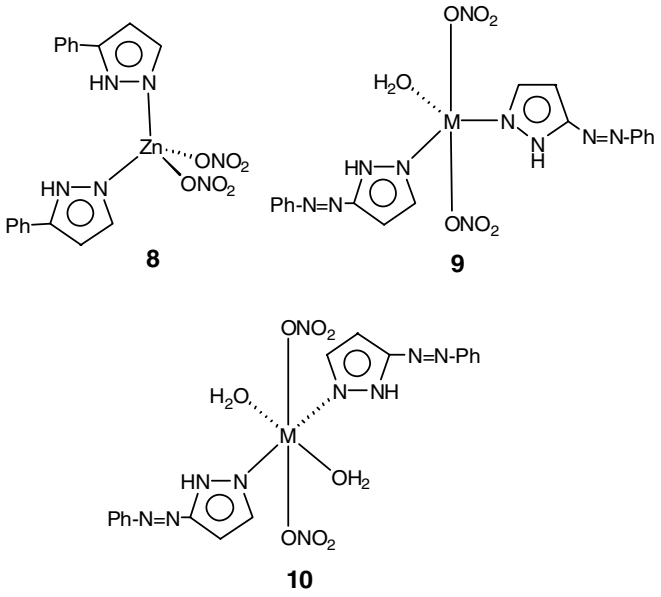

Scheme 5. Pyrazolato complexes **8**, **9**, and **10**.

2.8. Synthesis of [Zn(3-PhpzH)$_2$(NO$_3$)$_2$] (**8**)

$Zn(NO_3)_2 \cdot 6H_2O$ (0.04 g, 0.14 mmol) and 3-phenylpyrazole (0.04 g, 0.28 mmol) were combined in ethanol (10 mL) under ambient conditions, forming a clear colorless solution. Slow evaporation of the solvent led to deposition of colorless plates of **8**.

2.9. Synthesis of [Zn(4-PhN=NpzH)$_2$(NO$_3$)$_2$(H$_2$O)] (**9**)

$Zn(NO_3)_2 \cdot 6H_2O$ (0.04 g, 0.14 mmol) and 4-phenyldiazopyrazole [8] (0.05 g, 0.27 mmol) were combined in ethanol (10 mL) under ambient conditions, forming a clear red solution. Slow evaporation of the solvent led to deposition of red plates of product **9**.

2.10. Synthesis of [Cd(4-PhN=NpzH)$_2$(NO$_3$)$_2$(H$_2$O)$_2$] (**10**)

$Cd(NO_3)_2 \cdot 4H_2O$ (0.04 g, 0.14 mmol) and 4-phenyldiazopyrazole (0.048 g, 0.28 mmol) were combined in wet ethanol (10 mL) under ambient conditions, forming a clear red solution. Slow evaporation of the solvent led to deposition of red plates of product **10**.

2.11. Crystal structure determination

Data collection. STOE IPDS II two-circle diffractometer [**1**, **2**, **3**, **4**, [**Li**][**5**], [**6**][(**NO$_3$**)$_2$], **7**(**Co**), **7**(**Ni**), **7** (**Cu**), **7**(**Zn**), **7**(**Cd**),**8**, and **9**], Siemens-SMART-CCD three-circle diffractometer [**10**], graphite monochromated Mo Kα radiation ($\lambda = 0.71073$ Å), $T = 173(2)$ K. Empirical absorption corrections were performed using SADABS [9] [**10**] or the MULABS [10] option [**1**, **2**, **3**, **4**, [**Li**][**5**], [**6**][(**NO$_3$**)$_2$], **7** (**Co**), **7**(**Ni**), **7**(**Cu**), **7**(**Zn**), **7**(**Cd**), **8**, and **9**] in PLATON [11]. The structures were solved by direct methods using the program SHELXS [12] and refined against F^2 with full-matrix least-squares techniques using the program SHELXL-97 [13]. All non-hydrogen atoms were refined with anisotropic displacement parameters. Hydrogen atoms were located by difference Fourier synthesis and refined using a riding model.

3. Results and discussion

3.1. Deboronation of scorpionates

Recently, we have synthesized different types of homo- and heteroscorpionates [4,5,14–21]. As shown in Fig. 2,

Table 1
Selected bond lengths and angles of **7**(**Co**), **7**(**Ni**), **7**(**Cu**), **7**(**Zn**), and **7**(**Cd**)

Compound	**7**(**Co**)	**7**(**Ni**)	**7**(**Cu**)	**7**(**Zn**)	**7**(**Cd**)
M–N av. (Å)	2.1127(12)	2.0810(10)	2.0174(18)	2.1231(10)	2.3258(16)
M–O (Å)	2.1637(11)	2.1068(10)	2.3417(15)	2.1688(9)	2.3842(12)
M–O(1)–N(1) (°)	143.11(10)	138.68(9)	147.66(14)	143.08(8)	126.22(11)

Table 2
Crystallographic data of **1**, **2**, **3**, **4**, [**Li**][**5**], [**6**][$(NO_3)_2$], **7**(**Co**), **7**(**Ni**), **7**(**Cu**), **7**(**Zn**), **7** (**Cd**), **8**, **9**, and **10**

Compound	**1**	**2**	**3**	**4**	[**Li**][**5**]	[**6**][$(NO_3)_2$]	**7**(**Co**)
Formula	$C_{14}H_{24}C_{12}N_4Zn$	$C_{54}H_{48}C_{14}Fe_2N_{12}$	$C_{12}H_{16}Br_2CuN_8$	$C_{16}H_{18}C_{12}N_6Ni$	$C_{29}H_{53}C_{14}LiN_8O_4Ti_2$	$C_{54}H_{46}N_{14}O_6Zn_2$	$C_{36}H_{32}CoN_{10}O_6$
Formula weight	384.64	1118.54	495.69	423.97	822.33	1117.79	759.65
Color	colorless	colorless	blue	colorless	colorless	colorless	pink
Crystal size (mm)	$0.25 \times 0.15 \times 0.11$	$0.22 \times 0.21 \times 0.19$	$0.24 \times 0.18 \times 0.09$	$0.25 \times 0.23 \times 0.05$	$0.25 \times 0.24 \times 0.12$	$0.\ 26 \times 0.18 \times 0.14$	$0.38 \times 0.26 \times 0.12$
T (K)	100(2)	173(2)	173(2)	173(2)	173(2)	100(2)	100(2)
Radiation (Å)	0.71073	0.71073	0.71073	0.71073	0.71073	0.71073	0.71073
Crystal system	triclinic	monoclinic	monoclinic	monoclinic	monoclinic	monoclinic	triclinic
Space group	$P\bar{1}$	$P2_1/n$	$C2/c$	$P2_1/n$	$P2_1/n$	$C2/c$	$P\bar{1}$
a (Å)	9.541(3)	11.8555(18)	14.2274(16)	7.6754(6)	11.8715(8)	24.657(2)	7.7915(8)
b (Å)	9.719(3)	17.781(2)	9.3074(10)	16.0945(8)	23.145(2)	13.6400(10)	9.8735(10)
c (Å)	10.948(3)	12.8403(17)	14.4078(18)	15.5772(11)	14.9585(10)	16.4960(10)	12.5155(14)
α (°)	85.46(2)	90	90	90	90	90	71.718(8)
β (°)	89.82(2)	102.073(11)	118.176(8)	92.553(6)	95.741(5)	113.024(6)	76.695(8)
γ (°)	67.50(2)	90	90	90	90	90	75.676(8)
V (Å^3)	934.6(5)	2646.9(6)	1681.8(3)	1922.4(2)	4089.5(5)	5106.0(6)	873.53(16)
Z	2	2	4	4	4	4	1
D_{calc} (g cm^{-3})	1.367	1.403	1.958	1.465	1.336	1.454	1.444
$F(000)$	400	1152	972	872	1720	2304	393
μ (mm^{-1})	1.599	0.799	6.061	1.298	0.693	1.006	0.553
Minimum/maximum θ (°)	0.6907/0.8438	0.8438/0.8630	0.3240/0.6115	0.7373/0.9379	0.8458/0.9214	0.7800/0.8720	0.8172/0.9366
Number of reflections collected	3340	11003	1548	22608	21661	31041	12279
Number of independent reflections (R_{int})	3340	4874	1548	3600	7835	4908	4021
Number of data/restraints/parameters	3340/0/191	4874/0/337	1548/0/107	3600/0/234	7835/0/437	4908/0/351	4021/0/241
Goodness-of-fit on F^2	1.096	1.056	1.058	1.054	1.019	0.928	1.076
R_1, wR_2 [$I > 2\sigma(I)$]	0.0683, 0.1857	0.0652, 0.1531	0.0382, 0.1020	0.0308, 0.0638	0.0572, 0.1236	0.0453, 0.0917	0.0387, 0.1039
R_1, wR_2 (all data)	0.1132, 0.2279	0.0979, 0.1674	0.0422, 0.1050	0.0398, 0.0666	0.0931, 0.1379	0.0815, 0.1021	0.0401, 0.1051
Largest difference in peak and hole (e Å^{-3})	0.951 and −0.864	0.856 and −0.874	0.814 and −1.075	0.216 and −0.359	0.854 and −0.406	0.357 and −0.887	0.534 and −1.241

Compound	**7**(**Ni**)	**7**(**Cu**)	**7**(**Zn**)	**7**(**Cd**)	**8**	**9**	**10**
Formula	$C_{36}H_{32}N_{10}NiO_6$	$C_{36}H_{32}CuN_{10}O_6$	$C_{36}H_{32}N_{10}O_6Zn$	$C_{36}H_{32}CdN_{10}O_6$	$C_{18}H_{16}N_6O_6Zn$	$C_{18}H_{18}N_{10}O_7Zn$	$C_{18}H_{20}CdN_{10}O_8$
Formula weight	759.43	764.26	766.09	813.12	477.74	551.79	616.84
Color	blue	green	colorless	colorless	colorless	red	red
Crystal size (mm)	$0.38 \times 0.32 \times 0.28$	$0.28 \times 0.22 \times 0.11$	$0.46 \times 0.38 \times 0.32$	$0.27 \times 0.14 \times 0.08$	$0.31 \times 0.18 \times 0.07$	$0.35 \times 0.15 \times 0.14$	$0.16 \times 0.08 \times 0.06$
T (K)	100(2)	100(2)	100(2)	100(2)	100(2)	100(2)	147(2)
Radiation (Å)	0.71073	0.71073	0.71073	0.71073	0.71073	0.71073	0.71073
Crystal system	triclinic	triclinic	triclinic	triclinic	triclinic	monoclinic	monoclinic
Space group	$P\bar{1}$	$P\bar{1}$	$P\bar{1}$	$P\bar{1}$	$P\bar{1}$	$C2/c$	$P2_1/c$
a (Å)	7.7143(12)	7.9618(11)	7.7944(6)	7.9531(5)	7.8214(10)	25.689(2)	14.078(3)
b (Å)	9.8592(16)	9.8234(15)	9.8693(8)	9.8226(7)	15.6360(19)	10.3260(7)	8.3015(12)
c (Å)	12.425(2)	12.3207(19)	12.5030(10)	23.8269(17)	15.904(2)	8.5928(8)	10.130(3)
α (°)	72.792(13)	71.836(12)	71.962(6)	82.792(6)	86.370(10)	90	90
β (°)	77.420(13)	76.526(11)	76.707(6)	80.535(6)	89.577(11)	104.651(7)	93.646(15)
γ (°)	76.024(13)	74.898(11)	75.642(6)	80.535(6)	85.641(10)	90	90
V (Å^3)	865.0(2)	871.8(2)	873.63(12)	1766.9(2)	1935.5(4)	2205.3(3)	1181.5(4)
Z	1	1	1	2	4	4	2
D_{calc} (g cm^{-3})	1.458	1.456	1.456	1.528	1.640	1.662	1.734
$F(000)$	394	395	396	828	976	1128	620

(*continued on next page*)

Table 2 (*continued*)

Compound	7(Ni)	7(Cu)	7(Zn)	7(Cd)	8	9	10
μ (mm^{-1})	0.624	0.689	0.765	0.680	1.321	1.179	0.991
Minimum/maximum θ (°)	0.7975/0.8447	0.8305/0.9281	0.7198/0.7918	0.8378/0.9476	0.6850/0.9132	0.6830/0.8523	0.947/1.000
Number of reflections collected	13529	10459	19058	40541	15261	13076	10224
Number of independent reflections (R_{int})	3648	4098	4944	7630	6793	2603	2981
Number of data/restraints/parameters	3648/0/241	4098/0/241	4944/0/241	7630/0/494	6793/0/559	2603/0/172	2981/0/178
Goodness-of-fit on F^2	1.041	0.986	1.047	0.832	1.210	1.055	0.969
R_1, wR_2 [$I > 2\sigma(I)$]	0.0279, 0.0712	0.0396, 0.0640	0.0312, 0.0802	0.0229, 0.0430	0.1218, 0.2846	0.0203, 0.0527	0.0442, 0.0645
R_1, wR_2 (all data)	0.0294, 0.0721	0.0615, 0.0666	0.0316, 0.0804	0.0330, 0.0439	0.1431, 0.2916	0.0233, 0.0534	0.0949, 0.0741
Largest difference in peak and hole (e Å^{-3})	0.550 and −0.476	0.445 and −0.679	0.605 and −0.695	0.575 and −0.413	1.657 and −1.014	0.317 and −0.214	0.464 and −0.461

simple scorpionates have been prepared on the one hand, bitopic benzene- and ferrocene-based scorpionates have been established on the other hand.

In some reactions of the alkali metal or thallium scorpionates with metal salts MX_2, the formation of the corresponding transition metal–pyrazolato complexes has been observed. Obviously, in these cases deboronation was preferable to metathesis (see Scheme 1).

An important factor influencing the stability of scorpionates appears to be the degree of steric crowding around the boron center. The results of earlier studies [3] and investigations in our group show that scorpionates $\mathbf{RB(3\text{-}R'pz)_3^-}$ and $\mathbf{RB(3\text{-}R'pz)_3^-}$ decompose in the presence of transition metal salts much more easily when **R** and **R′** are bulky. We found that treatment of fluorenyl scorpionate [$C_{13}H_9B$-(3-*t*Bupz)$_3$Li(THF)] [4] with $ZnCl_2$ or of [$C_{13}H_9B$-(3-Phpz)$_3$Li(THF)] [4] with $FeCl_2$ led to the formation of the coordination compounds **1** and **2** as shown in Scheme 2.

Moreover, we observed that the ditopic scorpionate [*p*-C_6H_4(B*t*Bupz$_2$)$_2$][Li(THF)$_4$]$_2$ [5] with the bulky *t*Bu substituent on the boron center reacts with $CuBr_2$ or with Ni(py)$_2$Cl$_2$ to produce the corresponding pyrazolato complexes as depicted in Scheme 2.

Another reason for the deboronation of these scorpionates may be the difference in Lewis acidity of the metal center in MX_2 on the one side and of the boron center in the corresponding borane of pyrazolyl borate on the other side. Obviously, the stronger Lewis acid reacts with the pyrazolide anion.

Our studies show that the reaction of scorpionate [*p*-C_6H_4(B*t*Bupz$_2$)$_2$][Li(THF)$_4$]$_2$ [5] with Ti(NMe$_2$)$_2$Cl$_2$ led to the formation of dinuclear anion [**5**]$^-$. As shown in Scheme 3, a similar reaction was observed when [FcB(3-phpz)$_3$][Li(THF)] [6] was treated with Zn(NO$_3$)$_2$. Single crystals of the cationic dinuclear pyrazolato Zn complex were obtained from THF, whereas X-ray quality crystals of the anionic dinuclear pyrazolato Ti complex were grown from hexane at ambient temperature.

It is interesting to note that degradation reactions of scorpionates were preferred in the presence of nucleophilic halides. In our aim to reverse deboronation reactions of scorpionates, we decided to synthesize pyrazolato complexes with weakly coordinating anions such as nitrates.

3.2. Syntheses of pyrazolato transition metal nitrates

Pyrazolato complexes **7**(**Co**), **7**(**Ni**), **7**(**Cu**), **7**(**Zn**), and **7**(**Cd**) are easily accessible from the reaction of one equivalent of M(NO$_3$)$_2$ (M = Co, Ni, Cu, Zn, Cd) and four equivalents of 3-phenylpyrazole in ethanol (Scheme 4).

The syntheses of tetra-coordinate Zn compound **8** were conveniently achieved by the reaction of one equivalent Zn(NO$_3$)$_2$ with two equivalents of 3-phenylpyrazole [7]. Complexes [Zn(4-PhN=NpzH)$_2$(NO$_3$)$_2$(H$_2$O)] (**9**) and [Cd(4-PhN=NpzH)$_2$(NO$_3$)$_2$(H$_2$O)$_2$] (**10**) were synthesized by a similar route as shown for 3-phenylpyrazolato

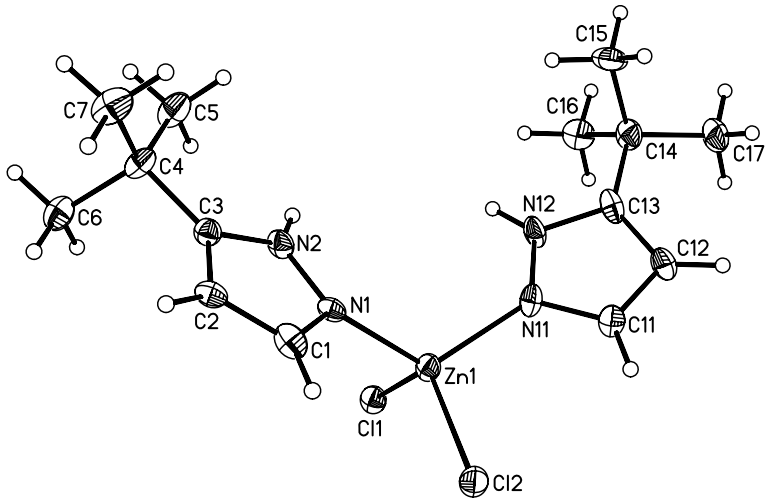

Fig. 3. Molecular structure of compound **1**; thermal ellipsoids shown at the 50% probability level. Selected bond lengths (Å) and angles (°): Zn(1)–N(11) 2.029(9), Zn(1)–N(1) 2.040(8), Zn(1)–Cl(2) 2.232(3), Zn(1)–Cl(1) 2.305(3), N(1)–C(1) 1.347(12), N(1)–N(2) 1.383(12), N(2)–C(3) 1.368(12), C(1)–C(2) 1.385(16), C(2)–C(3) 1.399(14), C(3)–C(4) 1.537(15), N(11)–C(11) 1.354(13), N(11)–N(12) 1.379(13), N(12)–C(13) 1.370(13), C(11)–C(12) 1.404(14), C(12)–C(13) 1.419(16), C(13)–C(14) 1.498(16); N(11)–Zn(1)–N(1) 117.8(4), N(11)–Zn(1)–Cl(2) 105.5(3), N(1)–Zn(1)–Cl(2) 106.7(2), N(11)–Zn(1)–Cl(1) 106.8(2), N(1)–Zn(1)–Cl(1) 105.6(3), Cl(2)–Zn(1)–Cl(1) 114.74(12), C(1)–N(1)–N(2) 105.6(8), C(1)–N(1)–Zn(1) 124.9(8), N(2)–N(1)–Zn(1) 128.3(6).

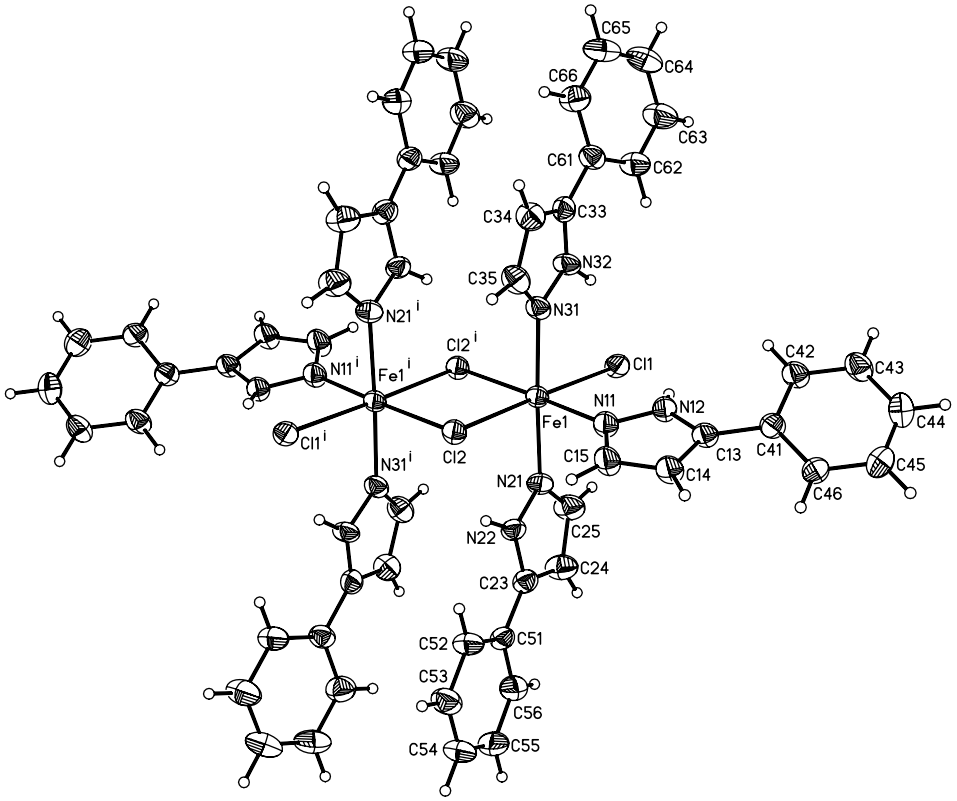

Fig. 4. Molecular structure of compound **2**; thermal ellipsoids shown at the 50% probability level. Selected bond lengths (Å) and angles (°): Fe(1)–N(31) 2.159(4), Fe(1)–N(21) 2.163(4), Fe(1)–N(11) 2.197, Fe(1)–Cl(1) 2.5131(13), Fe(1)–Cl(2)#1 2.5225(11), Fe(1)–Cl(2) 2.5641(13), Cl(2)–Fe(1)#1 2.5225(11), N(11)–C(15) 1.334(6), N(11)–N(12) 1.359(5), N(12)–C(13) 1.357(6), C(13)–C(14) 1.384(7), C(13)–C(41) 1.475(6), C(14)–C(15) 1.406(6), N(21)–C(25) 1.329(7), N(21)–N(22) 1.365(5), N(22)–C(23) 1.351(6), C(23)–C(24) 1.393(8), C(23)–C(51) 1.473(7), C(24)–C(25) 1.414(8), N(31)–C(35) 1.328(7), N(31)–N(32) 1.372(5), N(32)–C(33) 1.362(6), C(33)–C(34) 1.375(7), C(33)–C(61) 1.470(7), C(34)–C(35) 1.409(7), C(41)–C(42) 1.397(7), C(41)–C(46) 1.407(6), C(42)–C(43) 1.395(7), C(43)–C(44) 1.395(7), C(44)–C(45) 1.386(8), C(45)–C(46) 1.393(7), C(51)–C(56) 1.397(7), C(51)–C(52) 1.401(7), C(52)–C(53) 1.406(7), C(53)–C(54) 1.386(8), C(54)–C(55) 1.392(9), C(55)–C(56) 1.397(8), C(61)–C(66) 1.402(7), C(61)–C(62) 1.406(8), C(62)–C(63) 1.393(8), C(63)–C(64) 1.381(8), C(64)–C(65) 1.394(9), C(65)–C(66) 1.387(8); N(31)–Fe(1)–N(21) 177.07(14), N(31)–Fe(1)–N(11) 88.72(14), N(21)–Fe(1)–N(11) 88.41(14), N(31)–Fe(1)–Cl(1) 88.46(11), N(21)–Fe(1)–Cl(1) 90.90(11), N(11)–Fe(1)–Cl(1) 88.75(11), N(31)–Fe(1)–Cl(2)#1 90.52(10), N(21)–Fe(1)–Cl(2)#1 92.39(10), N(11)–Fe(1)–Cl(2)#1 175.71(11), Cl(1)–Fe(1)–Cl(2)#1 95.45(4), N(31)–Fe(1)–Cl(2) 91.87(11), N(21)–Fe(1)–Cl(2) 88.65(11), N(11)–Fe(1)–Cl(2) 88.79(11), Cl(1)–Fe(1)–Cl(2) 177.51(4), Cl(2)#1–Fe(1)–Cl(2) 87.02(4), Fe(1)#1–Cl(2)–Fe(1) 92.98(4). Symmetry transformations used to generate equivalent atoms: #1: $-x+1$, $-y+1$, $-z+1$.

transition metal complexes from 4-phenyldiazopyrazole [8] and $M(NO_3)_2$ (M = Zn, Cd) in ethanol at room temperature (Scheme 5).

Therefore, it can be concluded that complexes **7**(**Co**), **7**(**Ni**), **7**(**Cu**), **7**(**Zn**), **7**(**Cd**), **8**, **9**, and **10** possess a synthetic potential for the preparation of scorpionates. However, up to now our efforts to reverse the degradation reactions have not yet succeeded. So at 80 °C in the presence of Lewis bases such as NEt_3, reactions of aryldiaminioboranes and pyrazolato transition metal nitrates led to a cleavage of the C–B bond of aryldiaminoboranes [22].

3.3. X-ray crystallographic structures

The molecular structures of complexes **1**, **2**, **3**, **4**, [**Li**][**5**], [**6**][$(NO_3)_2$], **7**(**Co**), **7**(**Ni**), **7**(**Cu**), **7**(**Zn**), **7**(**Cd**), **8**, **9**, and **10** are shown in Figs. 3–14. Selected bond lengths and angles are listed in the corresponding figure captions and Table 1, details of the crystal structure analyses are summarized in Table 2.

In complexes **1**, **2**, **3**, **4**, **7**(**Co**), **7**(**Ni**), **7**(**Cu**), **7**(**Zn**), **7**(**Cd**), **8**, **9**, and **10**, pyrazole derivatives 3-R′pzH (R′ = H, *t*Bu, Ph) and 4-R′pzH (R′ = H, PhN=N) act as monodentate ligands, whereas in dinuclear anionic and cationic complexes, [**5**]$^-$ and [**6**]$^{2+}$, pyrazolide anions 3-R′pz$^-$ (R′ = H, Ph) act as bridging ligands.

Complex **1** crystallizes in the triclinic space group $P\bar{1}$ (Fig. 3). The Zn center in **1** is coordinated by two Cl atoms and two 3-*t*Bu-pyrazole molecules in a tetrahedral fashion.

The coordination geometry of the Fe atoms in **2** (monoclinic space group $P2_1/n$) is octahedral. The molecules form centrosymmetric dimers connected by two symmetry-related long axial Fe–Cl contacts of 2.5438(13) Å (Fig. 4). The Fe···Fe distance within the dimer is 3.689 Å. In the solid-state structure of dimeric **2**, two pyrazole molecules act as equatorial ligands and four pyrazole groups as axial ligands.

Fig. 5 shows the molecular structure of **3** (monoclinic space group $C2/c$). The Cu center in **3** is coordinated by four pyrazole groups and two bromide ions. The four pyrazole molecules in **3** are equatorially coordinated, the two bromide ions act as axial ligands. The Cu–Br bonds of 2.9976(5) Å are significantly longer than the Cu–Br bonds in the solid-state structure of $CuBr_2$.

As depicted in Fig. 6, the crystal structure of **4** (monoclinic space group $P2_1/n$) shows that all ligands in **3** are in a *trans* position. The average Ni–Cl distance in **3** of 2.4529(5) Å represents a characteristic value for Ni–Cl bonds.

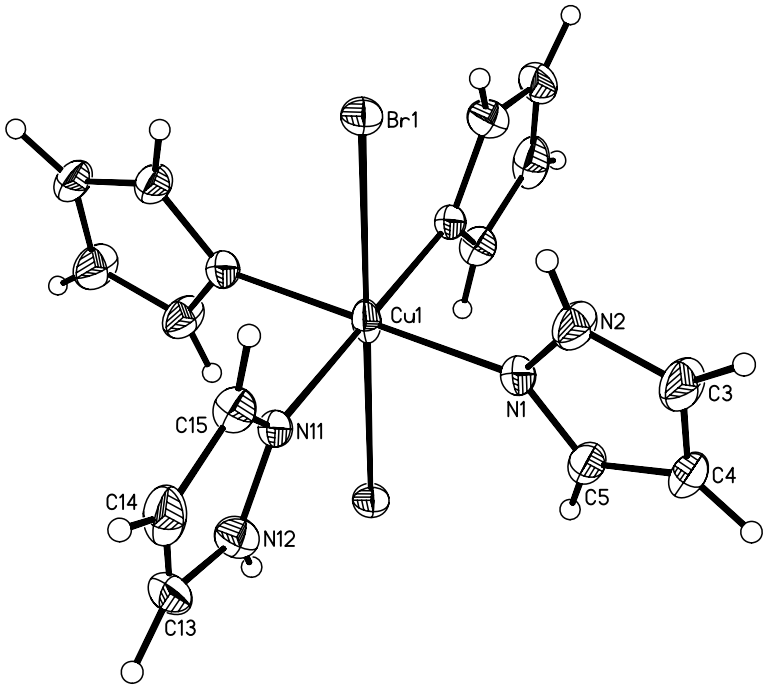

Fig. 5. Molecular structure of compound **3**; thermal ellipsoids shown at the 50% probability level. Selected bond lengths (Å) and angles (°): Cu(1)–N(1) 2.013(3), Cu(1)–N(1)#1 2.013(3), Cu(1)–N(11) 2.025(3), Cu(1)–N(11)#1 2.025(3), Cu(1)–Br(1)#1 2.9976(5), Cu(1)–Br(1) 2.9976(5), N(1)–C(5) 1.337(6), N(1)–N(2) 1.340(5), N(2)–C(3) 1.351(6), C(3)–C(4) 1.369(7), C(4)–C(5) 1.382(7), N(11)–C(15) 1.346(6), N(11)–N(12) 1.352(5), N(12)–C(13) 1.345(6), C(13)–C(14) 1.363(8), C(14)–C(15) 1.391(7); N(1)–Cu(1)–N(1)#1 179.998(1), N(1)–Cu(1)–N(11) 89.77(14), N(1)#1–Cu(1)–N(11) 90.22(14), N(1)–Cu(1)–N(11)#1 90.22(14), N(1)#1–Cu(1)–N(11)#1 89.78(14), N(11)–Cu(1)–N(11)#1 180.0(3), N(1)–Cu(1)–Br(1)#1 91.44(10), N(1)#1–Cu(1)–Br(1)#1 88.56(10), N(11)–Cu(1)–Br(1)#1 88.66(10), N(11)#1–Cu(1)–Br(1)#1 91.34(10), N(1)–Cu(1)–Br(1) 88.56(10), N(1)#1–Cu(1)–Br(1) 91.44(10), N(11)–Cu(1)–Br(1) 91.34(10), N(11)#1–Cu(1)–Br(1) 88.66(10), Br(1)#1–Cu(1)–Br(1) 180.0 Symmetry transformations used to generate equivalent atoms: #1: $-x+3/2$, $-y+3/2$, $-z+1$.

The structure of dinuclear anion $[\mathbf{5}]^-$ (monoclinic space group $P2_1/n$) is displayed in Fig. 7. The Ti centers in **Li**[**5**] are coordinated by three bridging pyrazolide ligands, two dimethylamido groups and four Cl atoms, forming a slightly distorted octahedron. The coordination geometry of the Ti atoms in the dinuclear anion $[\mathbf{5}]^-$ is octahedral. The Ti–N(1) [1.905(3) Å] and Ti–N(2) [1.906(4) Å] distances are short Ti–N single bonds. The Ti–Cl bonds of 2.3445(12) Å are comparable in length to the Ti–Cl bonds in titanium chloride derivatives. Fig. 8 illustrates the crystal packing of **Li**[**5**].

The dinuclear Zn complex [**6**][$(\mathbf{NO_3})_2$], shown in Fig. 9, crystallizes in the monoclinic $C2/c$ space group. The Zn atoms in [**6**][$(\mathbf{NO_3})_2$] are coordinated by two bridging 3-phenylpyrazolide ligands and two 3-phenylpyrazole molecules, forming a slightly distorted tetrahedron. It is interesting to note that the two moieties of the dinuclear cation in [**6**][$(\mathbf{NO_3})_2$] are also linked by hydrogen bridges via two NO_3^- anions.

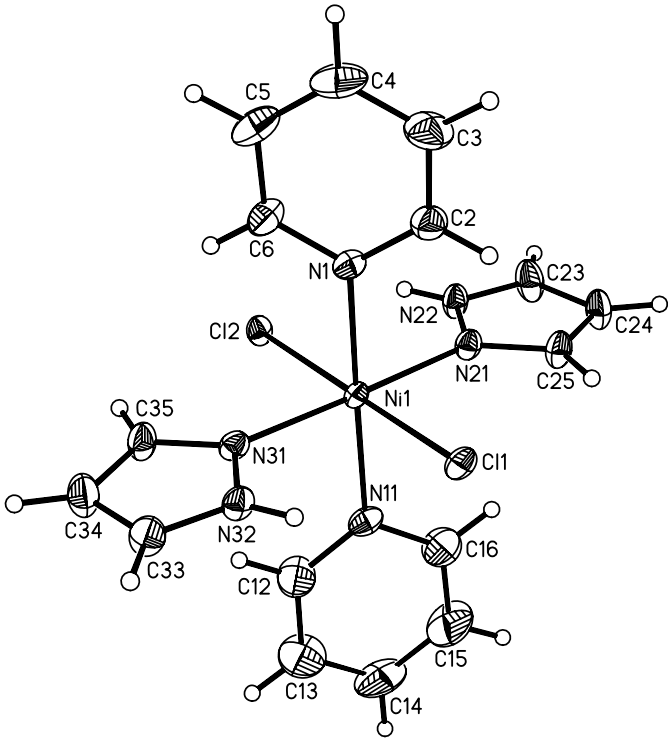

Fig. 6. Molecular structure of compound **4**; thermal ellipsoids shown at the 50% probability level. Selected bond lengths (Å), atom–atom distances (Å) and angles (°): Ni(1)–N(21) 2.0928(18), Ni(1)–N(31) 2.1095(18), Ni(1)–N(1) 2.1361(18), Ni(1)–N(11) 2.1793(18), Ni(1)–Cl(1) 2.4400(5), Ni(1)–Cl(2) 2.4658(5), N(1)–C(6) 1.345(3), N(1)–C(2) 1.346(3), C(2)–C(3) 1.390(3), C(3)–C(4) 1.384(4), C(4)–C(5) 1.381(4), C(5)–C(6) 1.389(3), N(11)–C(12) 1.337(3), N(11)–C(16) 1.342(3), C(12)–C(13) 1.394(4), C(13)–C(14) 1.377(5), C(14)–C(15) 1.367(5), C(15)–C(16) 1.388(4), N(21)–C(25) 1.343(3), N(21)–N(22) 1.350(3), N(22)–C(23) 1.344(3), C(23)–C(24) 1.380(3), C(24)–C(25) 1.398(3), N(31)–C(35) 1.338(3), N(31)–N(32) 1.357(2), N(32)–C(33) 1.344(3), C(33)–C(34) 1.379(3), C(34)–C(35) 1.402(3); N(21)–Ni(1)–N(31) 178.35(7), N(21)–Ni(1)–N(1) 89.04(7), N(31)–Ni(1)–N(1) 90.26(7), N(21)–Ni(1)–N(11) 90.84(7), N(31)–Ni(1)–N(11) 89.90(7), N(1)–Ni(1)–N(11) 178.40(7), N(21)–Ni(1)–Cl(1) 90.83(5), N(31)–Ni(1)–Cl(1) 90.66(5), N(1)–Ni(1)–Cl(1) 89.20(5), N(11)–Ni(1)–Cl(1) 89.20(5), N(21)–Ni(1)–Cl(2) 89.62(5), N(31)–Ni(1)–Cl(2) 88.88(5), N(1)–Ni(1)–Cl(2) 89.88(5), N(11)–Ni(1)–Cl(2) 91.72(5), Cl(1)–Ni(1)–Cl(2) 178.97(2).

Compounds **7**(**Co**), **7**(**Ni**), **7**(**Cu**), **7**(**Zn**), and **7**(**Cd**) are isostructural pyrazolato complexes. These compounds crystallize in the triclinic space group $P\bar{1}$ (Figs. 10 and 11). The unit cell dimensions of pyrazolato complexes **7**(**Co**), **7**(**Ni**), **7**(**Cu**), and **7**(**Zn**) are quite similar whereas those of **7**(**Cd**) differ somewhat. The metal atoms in **7**(**Co**), **7**(**Ni**), **7**(**Cu**), **7**(**Zn**), and **7**(**Cd**) have octahedral coordination geometries. The metal centers are coordinated by four 3-phenylpyrazole molecules and two NO_3^- anions. The two NO_3^- anions are in a *trans* position. In contrast to **7**(**Ni**), the ligand sphere of the Cu center in the solid-state structure of **7**(**Cu**) is thus considerably affected by a Jahn–Teller distortion. As shown in Table 1, complexes **7**(**Co**), **7**(**Ni**), **7**(**Cu**), **7**(**Zn**), and **7**(**Cd**) feature metal nitrogen distances with bond lengths between 2.0174(18) Å [**7**(**Cu**)] and 2.3258(16) Å [**7**(**Cd**)] and metal oxygen distances with bond lengths between 2.1068(10) Å [**7**(**Ni**)] and 2.3842(12) Å [**7**(**Cd**)].

Complex **8** crystallizes in the triclinic space group $P\bar{1}$ (Fig. 12). Zinc complex **8** shown in Fig. 12 (selected bond lengths and angles in the figure caption) crystallizes with two molecules in the asymmetric unit. The zinc ion in **8** is coordinated in a tetrahedral fashion by two 3-phenylpyrazole molecules [molecule **A**: Zn–N = 1.988(11) Å (av); molecule **B**: Zn–N = 1.991(11) Å (av)] and further by two NO_3^- anions [molecule **A**: Zn–O = 2.048(9) Å (av); molecule **B**: Zn–O = 2.029(9) Å (av)].

In the solid state, **9** (monoclinic space group $C2/c$) features a trigonal-pyramidally coordinated zinc center (Fig. 13). The Zn–O(1W) and Zn–N(1) bonds are equatorial and have Zn–O bond lengths of 1.9722(13) Å and Zn–N bond lengths of 2.0170(10) Å, while the Zn–O(1) bond of 2.1935(9) Å represents an axial bond (Fig. 14).

The solid-state structure of **10** shows that the Cd atom lies on a crystallographic inversion center. The Cd atom has octahedral coordination geometry. It is coordinated by two pyrazole groups, two nitrate groups and two water molecules. The azo group in **10** has a *trans* conformation. The angle between the plane of the pyrazole group and the plane of the azo group is 12.4°. The angle between the plane of the azo group and the plane of the phenyl ring is 17.5°. The shortest intramolecular contact distances are N(3)···H(5) 2.46 Å and O(3)···H(4B) 2.47 Å. The crystal packing shows intermolecular hydrogen bonding between the water molecules, pyrazole groups and nitrate anions. The crystal packing also features a weak intermolecular C–H···N interaction and intermolecular π···π interactions.

4. Supplementary data

Crystallographic data (excluding structure factors) for the structures reported in this paper have been deposited

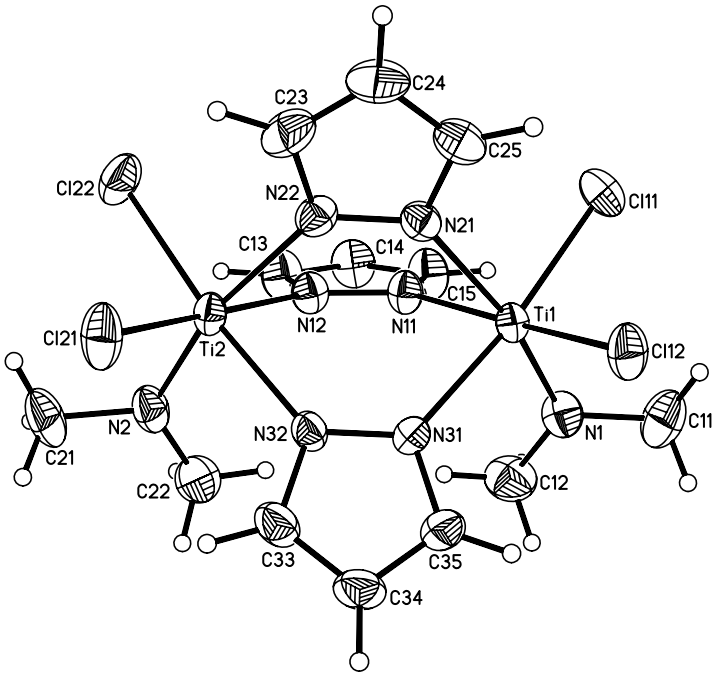

Fig. 7. Structure of the anion [**5**]; thermal ellipsoids shown at the 50% probability level. Selected bond lengths (Å) and angles (°): Ti(1)–N(1) 1.905(3), Ti(1)–N(31) 2.150(3), Ti(1)–N(11) 2.155(3), Ti(1)–N(21) 2.185(3), Ti(1)–Cl(11) 2.3427(12), Ti(1)–Cl(12) 2.3463(11), N(1)–C(11) 1.460(6), N(1)–C(12) 1.461(6), Ti(2)–N(2) 1.906(4), Ti(2)–N(12) 2.154(3), Ti(2)–N(32) 2.157(3), Ti(2)–N(22) 2.196(3), Ti(2)–Cl(21) 2.3496(11), Ti(2), Cl(22) 2.3525(12), N(2)–C(21) 1.469(5), N(2)–C(22) 1.470(6), N(11)–N(12) 1.365(4), N(11)–C(15) 1.367(5), N(12)–C(13) 1.351(5), C(13)–C(14) 1.378(6), C(14)–C(15) 1.377(6), N(21)–C(25) 1.352(5), N(21)–N(22) 1.368(4), N(22)–C(23) 1.350(5), C(23)–C(24) 1.384(7), C(24)–C(25) 1.379(6), N(31)–C(35) 1.356(5), N(31)–N(32) 1.366(4), N(32)–C(33) 1.364(5), C(33)–C(34) 1.371(6), C(34)–C(35) 1.380(6); N(1)–Ti(1)–N(31) 88.69(13), N(1)–Ti(1)–N(11) 88.46(14), N(31)–Ti(1)–N(11) 86.32(12), N(1)–Ti(1)–N(21) 168.56(14), N(31)–Ti(1)–N(21) 83.21(11), N(11)–Ti(1)–N(21) 82.99(12), N(1)–Ti(1)–Cl(11) 96.29(11), N(31)–Ti(1)–Cl(11) 173.30(9), N(11)–Ti(1)–Cl(11) 89.33(9), N(21)–Ti(1)–Cl(11) 91.21(9), N(1)–Ti(1)–Cl(12) 98.29(11), N(31)–Ti(1)–Cl(12) 90.72(8), N(11)–Ti(1)–Cl(12) 172.57(9), N(21)–Ti(1)–Cl(12) 89.91(8), Cl(11)–Ti(1)–Cl(12) 92.99(4), C(11), N(1)–C(12) 111.0(4), C(11)–N(1)–Ti(1) 120.8(3), C(12)–N(1)–Ti(1) 128.1(3), N(2)–Ti(2)–N(12) 88.15(13), N(2)–Ti(2)–N(32) 86.97(13), N(12)–Ti(2)–N(32) 86.44(12), N(2)–Ti(2)–N(22) 166.39(14), N(12)–Ti(2)–N(22) 82.82(12), N(32)–Ti(2)–N(22) 82.34(12), N(2)–Ti(2)–Cl(21) 96.86(11), N(12)–Ti(2)–Cl(21) 173.87(9), N(32)–Ti(2)–Cl(21) 90.29(8), N(22)–Ti(2)–Cl(21) 91.61(9), N(2)–Ti(2)–Cl(22) 98.43(11), N(12)–Ti(2)–Cl(22) 90.49(9), N(32), Ti(2)–Cl(22) 173.71(9), N(22)–Ti(2)–Cl(22) 91.84(9), Cl(21)–Ti(2)–Cl(22) 92.26(5), C(21)–N(2)–Ti(2) 120.6(3), C(22)–N(2)–Ti(2) 127.9(3), C(25)–N(21)–Ti(1) 123.7(3), N(22)–N(21)–Ti(1) 128.6(2), C(23)–N(22)–Ti(2) 123.7(3), N(21)–N(22)–Ti(2) 128.9(2), C(35)–N(31)–Ti(1) 122.4(3), N(32)–N(31)–Ti(1) 129.6(2), C(33)–N(32)–Ti(2) 123.4(3), N(31)–N(32)–Ti(2) 129.5(2).

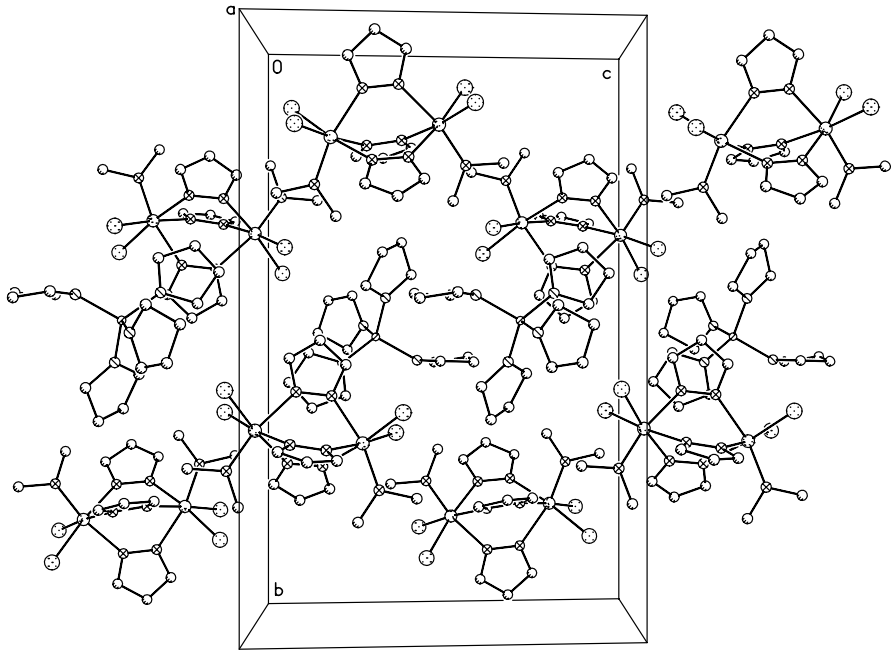

Fig. 8. Crystal packing diagram of compound [**Li**][**5**]; thermal ellipsoids shown at the 50% probability level.

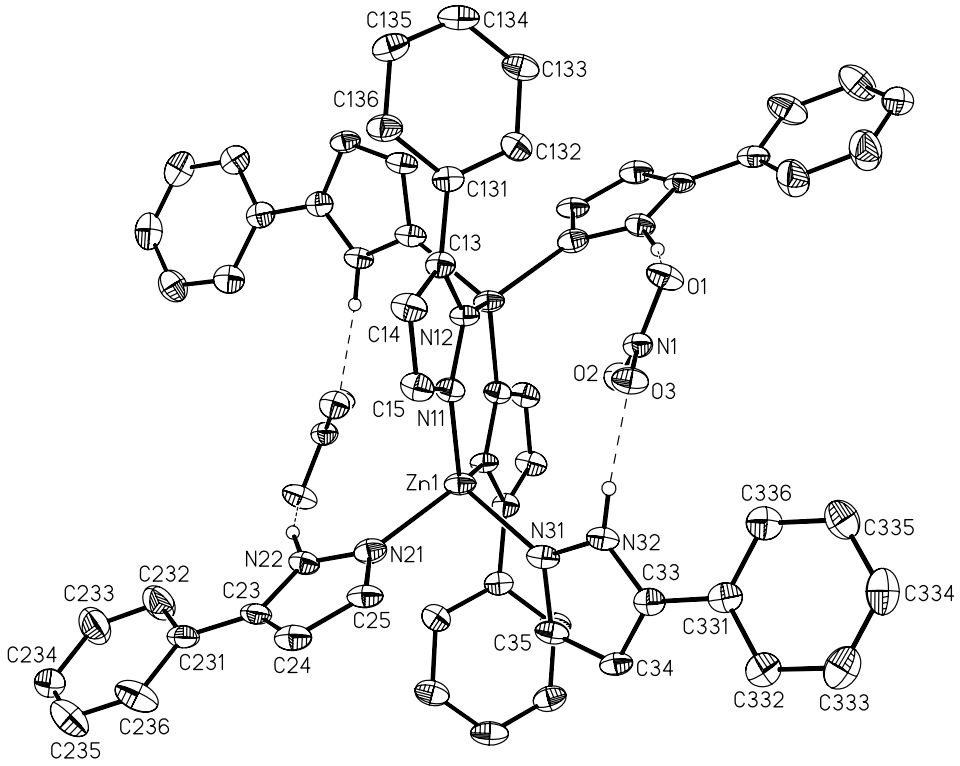

Fig. 9. Molecular structure of compound [**6**][$(NO_3)_2$]; thermal ellipsoids shown at the 50% probability level. Selected bond lengths (Å) and angles (°): Zn(1)–N(12)#1 1.974(3), Zn(1)–N(11) 1.987(3), Zn(1)–N(21) 2.058(3), Zn(1)–N(31) 2.058(3), N(11)–C(15) 1.346(4), N(11)–N(12) 1.390(4), N(12)–C(13) 1.369(4), N(12)–Zn(1)#1 1.975(3), C(13)–C(14) 1.391(5), C(13)–C(131) 1.482(4), C(14)–C(15) 1.393(5), N(21)–C(25) 1.348(4), N(21)–N(22) 1.372(4), N(22)–C(23) 1.362(4), N(22)–H(22) 1.01(6), C(23)–C(24) 1.397(5), C(23)–C(231) 1.476(5), C(24)–C(25) 1.396(5), N(31)–C(35) 1.357(4), N(31)–N(32) 1.364(4), N(32)–C(33) 1.347(4), N(32)–H(32) 0.86(4), C(33)–C(34) 1.391(5), C(33)–C(331) 1.479(5), C(34)–C(35) 1.395(5), C(131)–C(132) 1.399(5), C(131)–C(136) 1.405(5), C(132)–C(133) 1.399(5), C(133)–C(134) 1.392(6), C(134)–C(135) 1.391(6), C(135)–C(136) 1.398(5), C(231)–C(232) 1.386(6), C(231)–C(236) 1.397(5), C(232)–C(233) 1.384(6), N(1)–O(2) 1.255(4), N(1)–O(3) 1.263(4), N(1)–O(1) 1.269(4); N(12)#1–Zn(1)–N(11) 113.84(11), N(12)#1–Zn(1)–N(21) 125.61(12), N(11)–Zn(1)–N(21) 102.89(11), N(12)#1–Zn(1)–N(31) 107.16(11), N(11)–Zn(1)–N(31) 111.47(12), N(21)–Zn(1)–N(31) 94.06(11), C(15)–N(11)–N(12) 107.8(2), C(15)–N(11)–Zn(1) 124.1(2), N(12)–N(11)–Zn(1) 127.8(2), C(13)–N(12)–N(11) 107.5(3), C(13)–N(12)–Zn(1)#1 132.7(2), N(11)–N(12)–Zn(1)#1 118.18(19). Symmetry transformations used to generate equivalent atoms: #1: $-x+1/2$, $-y+3/2$, $-z+1$.

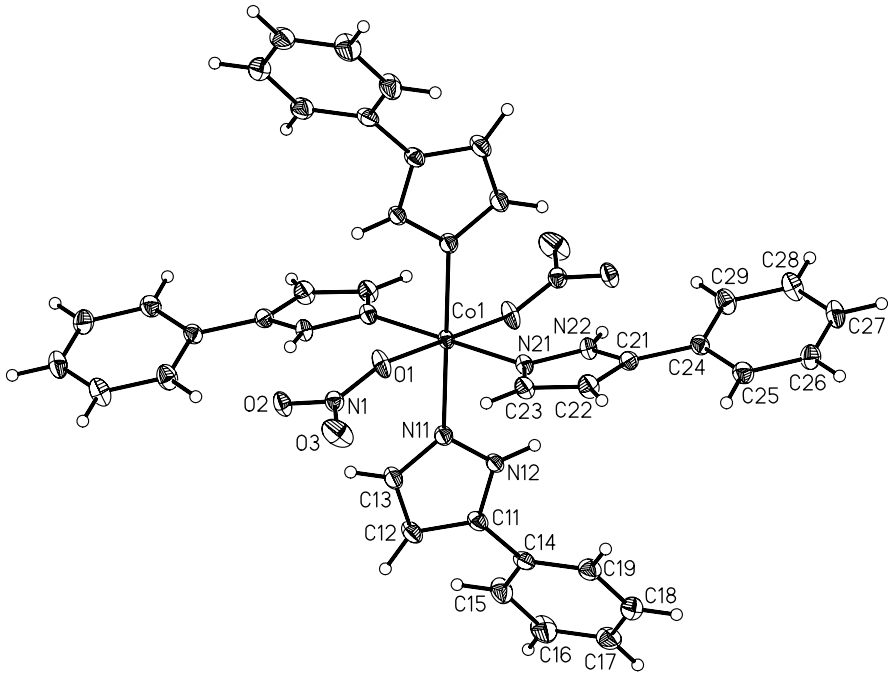

Fig. 10. Molecular structure of compound **7**(**Co**); thermal ellipsoids shown at the 50% probability level. **7**(**Co**), **7**(**Ni**), **7**(**Cu**), and **7**(**Zn**) are isostructural.

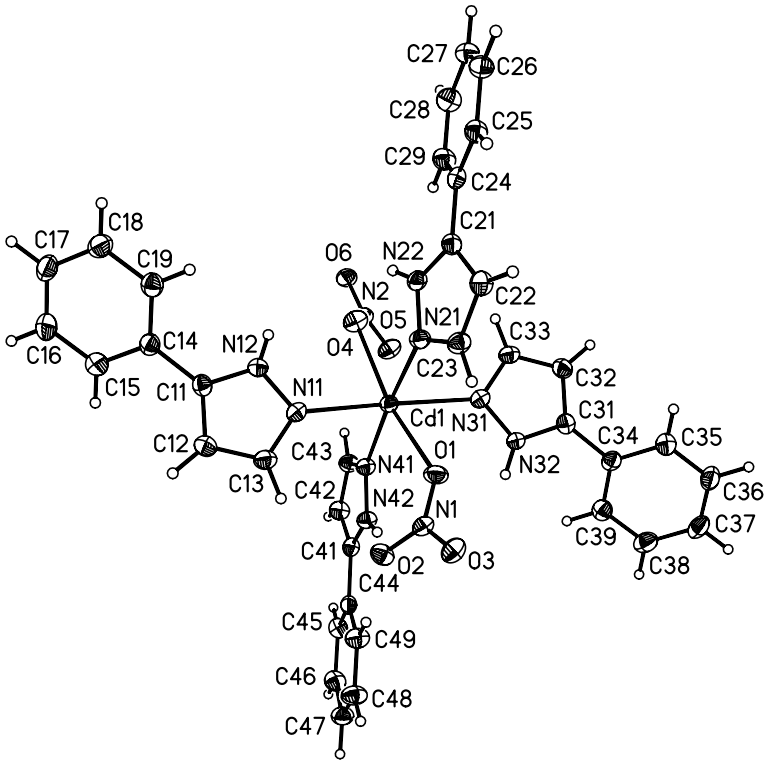

Fig. 11. Molecular structure of compound **7**(**Cd**); thermal ellipsoids shown at the 50% probability level.

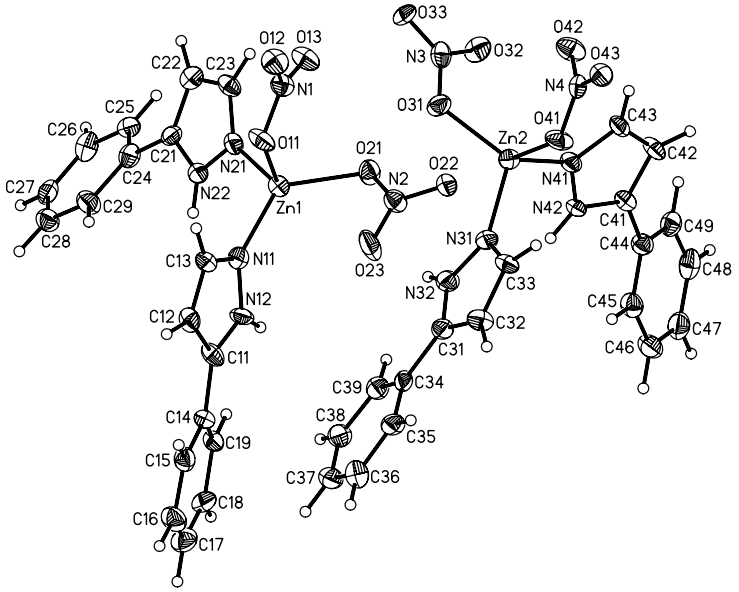

Fig. 12. Molecular structure of compound **8**; thermal ellipsoids shown at the 50% probability level. Selected bond lengths (Å), atom–atom distances (Å) and angles (°): Zn(1)–N(11) 1.983(11), Zn(1)–N(21) 1.992(11), Zn(1)–O(21) 2.033(9), Zn(1)–O(11) 2.062(9), Zn(1)–O(33)#1 2.534(8), Zn(2)–N(41) 1.966(11), Zn(2)–O(31) 2.003(9), Zn(2)–N(31) 2.012(11), Zn(2)–O(41) 2.055(9), Zn(2)–O(22) 2.527(9), N(1)–O(13) 1.238(14), N(1)–O(12) 1.252(14), N(1)–O(11) 1.304(14), N(2)–O(23) 1.242(14), N(2)–O(21) 1.247(14), N(2)–O(22) 1.248(13), N(3)–O(32) 1.218(14), N(3)–O(33) 1.241(13), N(3)–O(31) 1.299(14), N(4)–O(42) 1.213(14), N(4)–O(43) 1.244(13), N(4)–O(41) 1.268(14), N(11)–C(13) 1.351(16), N(11)–N(12) 1.376(15), N(12)–C(11) 1.354(16), C(11)–C(12) 1.388(17), C(11)–C(14) 1.480(18), C(12)–C(13) 1.367(18); N(11)–Zn(1)–N(21) 115.8(4), N(11)–Zn(1)–O(21) 124.7(4), N(21)–Zn(1)–O(21) 114.7(4), N(11)–Zn(1)–O(11) 89.1(4), N(21)–Zn(1)–O(11) 107.1(4), O(21)–Zn(1)–O(11) 96.6(4), N(11)–Zn(1)–O(33)#1 86.8(4), N(21)–Zn(1)–O(33)#1 79.5(4), O(21)–Zn(1)–O(33)#1 81.4(3), O(11)–Zn(1)–O(33)#1 173.3(4), N(41)–Zn(2)–O(31) 135.0(4), N(41)–Zn(2)–N(31) 114.9(4), O(31)–Zn(2)–N(31) 104.8(4), N(41)–Zn(2)–O(41) 103.0(4), O(31)–Zn(2)–O(41) 97.2(4), N(31)–Zn(2)–O(41) 89.8(4), N(41)–Zn(2)–O(22) 78.1(4), O(31)–Zn(2)–O(22) 82.7(3), N(31)–Zn(2)–O(22) 88.7(4), O(41)–Zn(2)–O(22) 178.5(3), O(13)–N(1)–O(12) 124.1(11), O(13)–N(1)–O(11) 120.8(10), O(12)–N(1)–O(11) 115.1(10), N(1)–O(11)–Zn(1) 118.6(7), O(23)–N(2)–O(21) 120.1(10), O(23)–N(2)–O(22) 120.2(11), O(21)–N(2)–O(22) 119.7(11), N(2)–O(21)–Zn(1) 111.7(7), N(2)–O(22)–Zn(2) 144.1(8), O(32)–N(3)–O(33) 123.6(11), O(32)–N(3)–O(31) 118.8(11), O(33)–N(3)–O(31) 117.6(10), N(3)–O(31)–Zn(2) 112.4(7), O(42)–N(4)–O(43) 123.5(11), O(42)–N(4)–O(41) 119.4(10), O(43)–N(4)–O(41) 117.1(10), N(4)–O(41)–Zn(2) 119.0(8). Symmetry transformations used to generate equivalent atoms: #1: $x-1$, y, z.

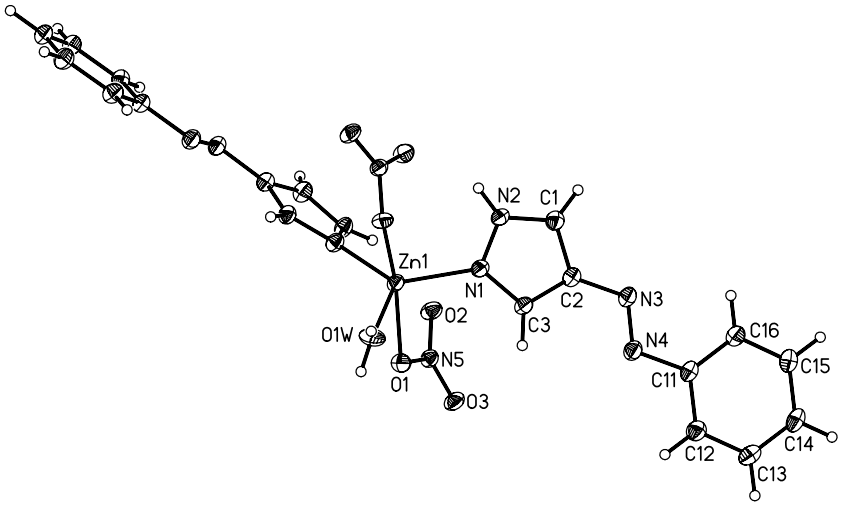

Fig. 13. Molecular structure of compound **9**; thermal ellipsoids shown at the 50% probability level. Selected bond lengths (Å), atom–atom distances (Å) and angles (°): Zn(1)–O(1W) 1.9722(13), Zn(1)–N(1) 2.0170(10), Zn(1)–N(1)#1 2.0170(10), Zn(1)–O(1)#1 2.1935(9), Zn(1)–O(1) 2.1935(9), N(1)–C(3) 1.3390(14), N(1)–N(2) 1.3558(14), N(2)–C(1) 1.3348(15), C(1)–C(2) 1.3833(17), C(2)–C(3) 1.4047(16), C(2)–N(3) 1.4090(14), N(3)–N(4) 1.2584(15), N(4)–C(11) 1.4334(15), C(11)–C(12) 1.3929(18), C(11)–C(16) 1.3962(17), C(12)–C(13) 1.3932(17), C(13)–C(14) 1.387(2), C(14)–C(15) 1.3936(19), C(15)–C(16) 1.3899(16), N(5)–O(3) 1.2322(13), N(5)–O(2) 1.2442(13), N(5)–O(1) 1.2967(13); O(1W)–Zn(1)–N(1) 119.64(3), O(1W)–Zn(1)–N(1)#1 119.64(3), N(1)–Zn(1)–N(1)#1 120.72(6), O(1W)–Zn(1)–O(1)#1 81.53(2), N(1)–Zn(1)–O(1)#1 98.51(4), N(1)#1–Zn(1)–O(1)#1 89.87(4), O(1W)–Zn(1)–O(1) 81.53(2), N(1)–Zn(1)–O(1) 89.87(4), N(1)#1–Zn(1)–O(1) 98.51(4), O(1)#1–Zn(1)–O(1) 163.06(4), C(3)–N(1)–N(2) 105.89(9), C(3)–N(1)–Zn(1) 130.16(8), N(2)–N(1)–Zn(1) 122.41(7), C(1)–N(2)–N(1) 111.86(10), C(1)–N(2)–H(2) 128.0(12), N(1)–N(2)–H(2) 120.2(12), O(3)–N(5)–O(2) 122.55(10), O(3)–N(5)–O(1) 118.91(10), O(2)–N(5)–O(1) 118.53(9), N(5)–O(1)–Zn(1) 114.37(7). Symmetry transformations used to generate equivalent atoms: #1: $-x+1$, y, $-z+3/2$.

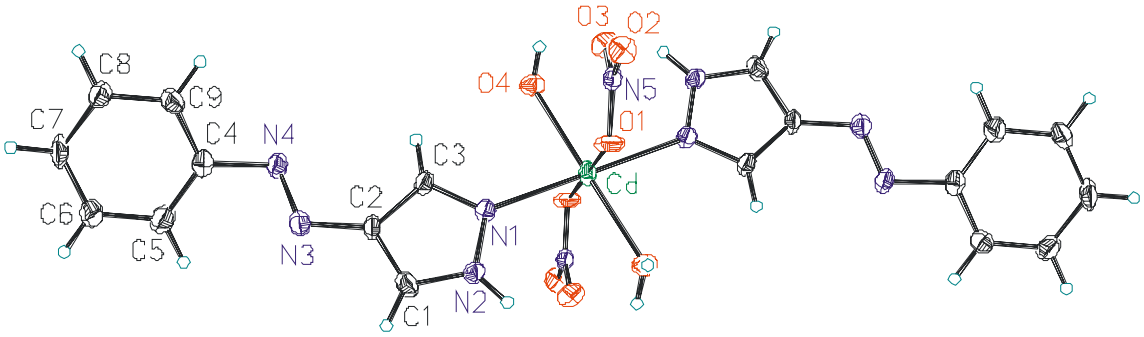

Fig. 14. Molecular structure of compound **10**; thermal ellipsoids shown at the 50% probability level. Selected bond lengths (Å), atom–atom distances (Å), angles (°) and torsion angles (°): Cd–N(1) 2.256(3), Cd–N(1)#1 2.256(3), Cd–O(4)#1 2.336(2), Cd–O(4) 2.336(2), Cd–O(1) 2.411(2), Cd–O(1)#1 2.411(2), O(2)–N(5) 1.239(3), O(1)–N(5) 1.273(3), N(3)–N(4) 1.249(3), N(3)–C(2) 1.406(4), O(3)–N(5) 1.243(3), N(2)–C(1) 1.334(4), N(2)–N(1) 1.358(3), N(4)–C(4) 1.444(4), C(3)–N(1) 1.327(4), C(3)–C(2) 1.409(4), C(2)–C(1) 1.370(4), C(4)–C(5) 1.366(5), C(4)–C(9) 1.374(5), C(9)–C(8) 1.388(4), C(7)–C(6) 1.369(5), C(7)–C(8) 1.379(5), C(6)–C(5) 1.382(5); N(1)–Cd–N(1)#1 180.0, N(1)–Cd–O(4)#1 92.19(9), N(1)#1–Cd–O(4)#1 87.81(9), N(1)–Cd–O(4) 87.81(9), N(1)#1–Cd–O(4) 92.19(9), O(4)#1–Cd–O(4) 180.0, N(1)–Cd–O(1) 85.68(9), N(1)#1–Cd–O(1) 94.32(9), O(4)#1–Cd–O(1) 74.11(10), O(4)–Cd–O(1) 105.89(10), N(1)–Cd–O(1)#1 94.32(9), N(1)#1–Cd–O(1)#1 85.68(9), O(4)#1–Cd–O(1)#1 105.89(10), O(4)–Cd–O(1)#1 74.11(10), O(1)–Cd–O(1)#1 180.0, N(5)–O(1)–Cd 109.90(18), N(4)–N(3)–C(2) 114.4(3), O(2)–N(5)–O(3) 121.8(3), O(2)–N(5)–O(1) 119.5(3), O(3)–N(5)–O(1) 118.8(3), C(1)–N(2)–N(1) 111.7(3), N(3)–N(4)–C(4) 112.6(3), N(1)–C(3)–C(2) 110.6(3), C(3)–N(1)–N(2) 105.3(2), C(3)–N(1)–Cd 130.7(2), N(2)–N(1)–Cd 123.93(19). Symmetry transformations used to generate equivalent atoms: #1: $-x+1$, $-y$, $-z$.

with the Cambridge Crystallographic Data Centre as supplementary publication Nos. CCDC 282886 [**1**], CCDC 282889 [**2**], CCDC 282888 [**3**], CCDC 282887 [**4**], CCDC 282890 [**Li**][**5**], CCDC 283070 [**6**][$(NO_3)_2$], CCDC 282881 [**7**(**Co**)], CCDC 282880 [**7**(**Ni**)], CCDC 282882 [**7**(**Cu**)], CCDC 282883 [**7**(**Zn**)], CCDC 282885 [**7**(**Cd**)], CCDC 282879 [**8**], CCDC 282884 [**9**], and CCDC 283003 [**10**]. Copies of the data can be obtained free of charge on application to CCDC, 12 Union Road, Cambridge CB2 1EZ, UK (fax: +44 1223 336 033; e-mail: deposit@ccdc.cam.ac.uk).

Acknowledgements

We are grateful to the University of Frankfurt for financial funding. M.W. is grateful to the "Deutsche Forschungsgemeinschaft" (DFG) for financial support.

References

[1] S. Trofimenko, Chem. Rev. 93 (1993) 943.
[2] R.D. Adams, F.A. Cotton (Eds.), Catalysis by Di- and Polynuclear Metal Cluster Complexes, Wiley, New York, 1988.
[3] O. Graziani, L. Toupet, J.-R. Hamon, M. Tilset, Inorg. Chim. Acta 341 (2002) 127.
[4] S. Bieller, M. Bolte, H.-W. Lerner, M. Wagner, J. Organomet. Chem. 690 (2005) 1935.
[5] S. Bieller, F. Zhang, M. Bolte, J.W. Bats, H.-W. Lerner, M. Wagner, Organometallics 23 (2004) 2107.
[6] S.L. Guo, F. Peters, F. Fabrizi de Biani, J.W. Bats, E. Herdtweck, P. Zanello, M. Wagner, Inorg. Chem. 40 (2001) 4928.
[7] A. Haghiri, H.-W. Lerner, M. Wagner, J.W. Bats, Acta Crystallogr., Sect. E 58 (2002) o1378.
[8] S.L. Guo, A. Haghiri, H.-W. Lerner, M. Wagner, unpublished work.
[9] G.M. Sheldrick, SADABS, University of Göttingen, Göttingen, Germany, 2000.
[10] R.H. Blessing, Acta Crystallogr., Sect. A 51 (1995) 33.
[11] A.L. Spek, Acta Crystallogr., Sect. A 46 (1990) C34.
[12] G.M. Sheldrick, Acta Crystallogr., Sect. A 46 (1990) 467.
[13] G.M. Sheldrick, SHELXL-97: A Program for the Refinement of Crystal Structures, University of Göttingen, Göttingen, Germany, 1997.
[14] A. Haghiri Ilkhechi, J.M. Mercero, I. Silanes, M. Bolte, M. Scheibitz, H.-W. Lerner, J.M. Ugalde, M. Wagner, J. Am. Chem. Soc. 127 (2005) 10656.
[15] A. Haghiri Ilkhechi, M. Bolte, H.-W. Lerner, M. Wagner, J. Organomet. Chem. 690 (2005) 1971.
[16] A. Haghiri Ilkhechi, S. Guo, M. Bolte, M. Wagner, Dalton Trans. (2003) 2303.
[17] F. Zhang, M. Bolte, H.-W. Lerner, M. Wagner, Organometallics 23 (2004) 5075.
[18] S.L. Guo, J.W. Bats, M. Bolte, M. Wagner, J. Chem. Soc., Dalton Trans. (2001) 3572.
[19] E. Herdtweck, F. Peters, W. Scherer, M. Wagner, Polyhedron 17 (1998) 1149.
[20] F. Fabrizi de Biani, F. Jäkle, M. Spiegler, M. Wagner, P. Zanello, Inorg. Chem. 36 (1997) 2103.
[21] F. Jäkle, K. Polborn, M. Wagner, Chem. Ber. 129 (1996) 603.
[22] L. Kaufmann, Diploma thesis, University of Frankfurt, Germany, 2005.